EPR study of defect reorientation by a tunneling-controlled process

M. L. Sanjuán, V. M. Orera, and P. J. Alonso
Instituto de Ciencia de Materiales de Aragón, Universidad de Zaragoza—Consejo Superior de Investigaciones Científicas, Facultad de Ciencias, 50009 Zaragoza, Spain
(Received 28 March 1990)

By means of EPR, we have studied the problem of an anisotropic paramagnetic defect in a double potential well, which reorients either by tunneling in the ground state or via thermal excitation to higher states. The EPR spectrum is simulated by means of the stochastic Liouville equation as a function of parameters such as jump probabilities, transition rates to the excited state, etc. Perturbative solutions are discussed for the simplest secular spin-Hamiltonian case in limit situations. Computer simulations are presented for other cases of practical interest. The method is then used to study the reorientation of the H_i^0(Li) and D_i^0(Li) defects in CaO from the static to the extreme-narrowing regimes. Good agreement is found between calculated and experimental spectra. Reorientation and excitation frequencies are obtained from the fitting.

I. INTRODUCTION

Electron paramagnetic resonance (EPR) has been widely used to obtain information about the dynamic behavior of paramagnetic entities. In recent years we have applied this technique to the study of the reorientation of small molecules and defects in crystals.[1–3]

The existence of a dynamic process affects the EPR spectra. In the case of a reorienting spin system having anisotropic interactions, the EPR lines go through broadening, coalescence, and narrowing regimes as the reorientation rate increases. The dynamic process can be described by parameters such as hopping frequencies which can be obtained from the EPR measurements.

The procedure is based on the comparison between the experimental spectra at different temperatures and those calculated as a function of the reorientation frequency. We have used a line-shape-simulation method based on the stochastic-Liouville-equation (SLE) formalism. It has the advantage over other methods, such as those derived from the Bloch equations or the relaxation matrix, of being valid in the entire reorientation frequency range and suitable for handling pseudoscalar and nonsecular interactions.

In order to apply the method, it is necessary to have a good knowledge of both the magnetic interactions and the jumping process. The magnetic interactions of the spin system are described by a spin Hamiltonian, whose parameters can be deduced from the EPR rotational diagram in the static situation. The reorientation mechanisms are in general thermally activated jumps between ground states of the defect in different potential wells. The hopping rates are thus described by a reorientation frequency that stands for the defect average residence time in each well. The dynamic jump matrix can be easily obtained.

However, we have recently studied two defects, the H_i^0(Li) in CaO and its deuterated form D_i^0(Li), whose dynamic behavior departs from the general trend.[4] In order to explain the experimental observations, we have proposed a mechanism similar to the well-known tunneling-controlled process[5,6] in which the reorientation of the defects would take place through tunneling between the first-excited vibrational states.

Due to the difficulty of handling different dynamic contributions superimposed on the same system, the analysis that we did in Ref. 4 was limited to a qualitative explanation of the experimental results, exception made of the high-temperature situation where the results of the relaxation matrix theory hold.

In the present paper we apply the SLE method to that problem. The calculations fit quite well the experimental behavior of the H_i^0(Li) and D_i^0(Li) defects in CaO. In fact, the existence of fast phonon-induced transitions between the ground and the excited levels, and of a fast reorientation rate among the excited levels, accounts for the unexpectedly large hopping rates at low temperatures and for the observed inverse isotopic effect. This model also explains why the widths of the hyperfine lines are not uniform in the narrowing regime.

The model could also be applied to other situations: for instance, when the excited levels are not of vibrational type as in the case of motion of nitrogen in silicon between on-center and off-center configurations,[7] when tunneling between ground states is important, or when reorientation is negligible as compared with thermal excitation. Therefore we present general solutions which are also valid for these cases.

The paper is organized as follows. In Sec. II we develop the main assumptions of the model and define the parameters of the system. In Sec. III we summarize the line-shape theory and Liouville formalism as they apply to our problem. Some perturbative solutions are presented in Sec. III B for limit situations in which effective parameters can be defined. In Sec. III C complete computer simulations are shown for cases of general interest. Though the method is of wide applicability, in order to illustrate typical behavior at the different dynamic stages

we refer throughout the paper to the particular case of H_i^0(Li) and D_i^0(Li) in CaO. In Sec. IV we undertake the study of these two defects in more detail. The results are finally discussed in the last section where some conclusions are also presented.

II. DYNAMIC MODEL

Before we start with line-shape simulations it is useful to define the processes and parameters entering our problem: We have a paramagnetic defect which can occur in two (or more) sites that are magnetically inequivalent, i.e., they yield different EPR spectra. Both sites are connected through a potential barrier that is so high that at very low temperatures the defect is localized in its ground state in one site, the tunneling or hopping rate between both sites being extremely low.

For a three-dimensional harmonic-type potential well, there are excited states in which the defect oscillates with energies $(n+\frac{3}{2})h\nu$. The harmonic assumption is not essential in our model, and we will consider just one excited state in each well, triply degenerate, at energy Δ from the fundamental state. If $kT \ll \Delta$ the population of the excited state will be negligible and there is no need to consider it. This may be the case, for instance, for the H_i^0(Li) and D_i^0(Li) defects in MgO.[3] However, if kT and Δ are of the same order of magnitude that approximation is not valid.

We will label the levels 1,2,3,4 as in Fig. 1. These levels are split by the magnetic field and their EPR resonance frequencies are $\omega_1,\omega_2,\omega_3,\omega_4$. The quantities $\delta_0=\omega_1-\omega_3$ and $\delta_e=\omega_2-\omega_4$ represent the anisotropy of the ground and excited states, respectively.

Four types of dynamic processes can affect the EPR spectra.

(1) Vibration of the defect in a harmonic-oscillator (HO) type level "n," with frequency ν_n. This mechanism adds a dynamic contribution to the hyperfine interaction and explains, for instance, the direct isotope effect in the isotropic lithium superhyperfine (shf) parameter of H_i^0(Li) and D_i^0(Li) in MgO and CaO ($M_D > M_H \rightarrow a_{Li}[D_i^0(Li)] < a_{Li}[H_i^0(Li)]$ for the same HO level). When comparing different levels in the same site we expect that $a_i > a_j$ if $n_i > n_j$.[4]

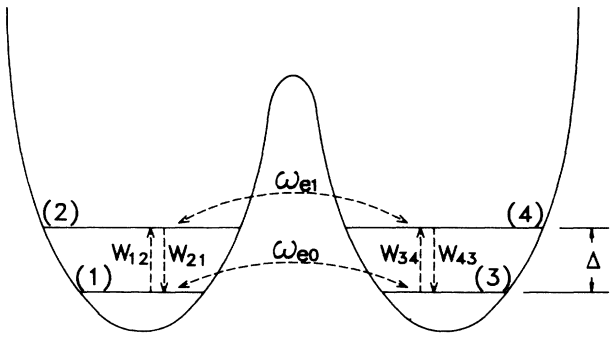

FIG. 1. Labeling of states in a double-potential-well model and parameters involved.

(2) Thermal excitation and deexcitation between vibrational levels within one well ($1\leftrightarrow2$, $3\leftrightarrow4$). Through this mechanism the defect performs fast transitions from, say, level 1 to 2 and back, at rates W_{12} and W_{21}, respectively. From the thermal equilibrium condition we have $W_{21}/W_{12}=\exp(\Delta/kT)$ and the same for levels 3 and 4. Following Ref. 8, we assume for W_{12} a dependence of the form $W_{12}=Kn_0(\Delta,T)$ where $n_0(\Delta,T)$ is the Bose-Einstein factor and K is a constant including that part of the defect-lattice interaction causing the thermal excitation. These processes are very fast, occurring with frequencies of the order of the phonon ones.

(3) Reorientation from one site to the other, either in the ground state ($1\leftrightarrow3$) or in the excited state ($2\leftrightarrow4$). The probability of tunneling will be characterized by rates ω_{e0} and ω_{e1} in the ground and excited states, respectively. Localization in the ground state takes place, since the tunneling matrix element for that level is expected to be smaller than the energy separation of the two orientation states caused by lattice relaxation.

In the case of the excited state the situation is not so clearly defined, since we do not have direct experimental access to the averaging stage in that level. Thus the degree of localization in the excited state is unknown. However, since the barrier height is smaller, one might expect the reorientation frequency to be much higher than in the ground state. A study of the tunneling probability taking into account the level widths can be found in Ref. 6. Lifetime broadening added to misfitting between levels due to stresses diminishes the tunneling probability. So, in general the reorientation processes are quite slow ($\approx$MHz) when compared with the relaxations toward equilibrium given in the previous paragraph, but can be fast enough to produce an averaging of the magnetic anisotropy. A typical situation will be $\omega_{e0} \ll |\omega_1-\omega_3|$, while $\omega_{e1} \gg |\omega_2-\omega_4|$.

(4) Spin-lattice relaxation (SLR). This process, caused by the time modulation of the spin-orbit interaction, contributes to the EPR linewidth and is very significant in saturation effects. There exists a dependence of the spin-lattice lifetime with the tunneling process, but since in our case the contribution of the SLR to the spectra is small, we will neglect this effect.

III. LINE-SHAPE SIMULATIONS

We have performed line-shape simulations of the EPR spectra for the general case described in Sec. II. The stochastic Liouville formalism is based on the solution of the dynamic equation of the density matrix operator, ρ_s, for the spin system. The method has been described in previous papers[1-3] so that we will only mention the particularities that apply to this work.

The EPR spectrum is given by

$$P=\omega H_1 N h\bar{g}\beta \,\mathrm{Im}\{\mathrm{tr}[\rho(t)S_+]e^{-i\omega t}\} ,$$

where H_1 is the intensity of the microwave field, ω is the frequency of the microwave field, N is the number of spins, $\bar{g}$ is one-third of the trace of the $\tilde{g}$ matrix, $\rho(t)$ is the total density matrix (defect plus lattice) and the trace

applies to the degrees of freedom of both systems.

In the SLE method this equation yields

$$P=\omega H_1 N h\bar{g}\beta \mathrm{Im}\sum_{j=1}^{r}\mathrm{tr}_s[Z_j^{(1)}(\omega)S_+]\ ,$$

where r is the number of equivalent orientations of the defect, $Z_j^{(1)}(\omega)$ is the first harmonic of $\chi_j(t)=\sum_j e^{in\omega t}Z_j^{(n)}(\omega)$, $\chi_j(t)$ being the deviation from the equilibrium density matrix of the spin system (ρ_s^0) in site j.

In the absence of saturation $Z_j^{(1)}(\omega)$ is obtained by resolution of the following set of equations:

$$in\omega Z_j^{(1)}=-i[H_s+H_j,Z_j^{(1)}]+(\tilde{T}Z^{(1)})_j + \tilde{R}Z_j^{(1)}-id[S_-,\rho_s^0]\ , \quad (1)$$

where H_s is the average of the spin Hamiltonian (SH) over the r sites, H_j is the departure from H_s of the SH in site j and $d=g\beta H_1$. $\tilde{T}$ is the "transition matrix," which can be decomposed as $\tilde{T}=\tilde{\Gamma}+\tilde{K}$, with $\tilde{\Gamma}$ defined in such a way that its element Γ_{ji} represents the probability per unit time of the defect hopping from site i to site j (Γ_{ij} is proportional to the ω_e's defined above) and $\tilde{K}$ contains the transition probability from the ground to the excited state and vice versa, within each well. $\tilde{R}$ is the relaxation matrix. In the absence of saturation it can be substituted by a diagonal matrix with elements $R_{ij}=(1/T_2)\delta_{ij}$, T_2 being a relaxation time giving the "intrinsic linewidth." Finally,

$$\rho_s^0=\exp(-H_s/kT)/\mathrm{tr}[\exp(-H_s/kT)]\ .$$

Equation (1) is written and solved in an appropriate basis, according to the particular spin Hamiltonian considered. The static spectrum provides the spin-Hamiltonian parameters and intrinsic linewidth. From the fitting of the calculated spectra to the experimental ones the temperature evolution of the jump probability ω_e can be obtained.

A. Secular approximation

Very often, only diagonal Hamiltonian terms need to be retained, so that the dimension of the problem is considerably reduced. If there are hyperfine lines, for instance, each line will be separated from the others in this approach and we only need to solve a reduced equation for each line, of the form

$$\tilde{O}\mathbf{Z}=\mathbf{v}\ , \quad (2)$$

where $\tilde{O}$ is the Liouville operator (LO) for that specific line and $\mathbf{Z}$ and $\mathbf{v}$ are four-dimensional vectors: $\mathbf{Z}=(Z_1,Z_2,Z_3,Z_4)$, $\mathbf{v}=(v_1,v_2,v_3,v_4)$. The intensity vector $\mathbf{v}=d/Z[S_-,\exp(-H_s/kT)]$ has elements proportional to $(1,\eta\exp(-\Delta/kT),1,\eta\exp(-\Delta/kT))$ where the degeneracy η has been equal to 3. The notation 1, 2, 3, 4 applies to the labeling of Fig. 1. Some care must be taken with this degeneracy: W_{12} stands for the transition probability to each of the three excited-state sublevels. Assuming that all of them are equivalent the total transition probability from the ground to the excited state will be $3W_{12}$. On the contrary, ω_{e1} means the jump probability in the excited state as a whole, independently of its degeneracy.

Each LO has the form

$$\tilde{O}=\delta_{ij}(\omega-i/T_2)+\begin{bmatrix} -\omega_1-i3W_{12}-i\omega_{e0} & iW_{12}\exp(\Delta/kT) & i\omega_{e0} & 0 \\ i3W_{12} & -\omega_2-iW_{12}\exp(\Delta/kT)-i\omega_{e1} & 0 & i\omega_{e1} \\ i\omega_{e0} & 0 & -\omega_3-i3W_{12}-i\omega_{e0} & iW_{12}\exp(\Delta/kT) \\ 0 & i\omega_{e1} & i3W_{12} & -\omega_4-iW_{12}\exp(\Delta/kT)-i\omega_{e1} \end{bmatrix},$$

where all the quantities have been defined above and it has been assumed that $W_{34}=W_{12}$, $W_{43}=W_{21}=W_{12}\exp(\Delta/kT)$.

This matrix is diagonalized and then inverted. The static positions $\omega_1,\omega_2,\omega_3,\omega_4$ and intrinsic linewidth $1/T_2$ are obtained from the low-temperature spectrum. ω and T are known from the experiment conditions. Then, only four parameters play a role in the simulations: the tunneling probabilities ω_{e0}, ω_{e1}, the energy gap Δ, and the probability of the vibrational excitation W_{12}. Except Δ, all the others are a function of temperature.

B. Perturbative solutions

Usually, vibrational excitation is the fastest process so that we can follow a perturbative scheme as follows.

(1) First we diagonalize the transition matrix in the absence of reorientation ($W_{12},W_{21}\gg\omega_{e0},\omega_{e1}$). We define $p=W_{12}$ and $e=\exp(\Delta/kT)$:

$$K=\begin{bmatrix} -i3p & ipe & & \\ i3p & -ipe & & \\ & & -i3p & ipe \\ & & i3p & -ipe \end{bmatrix}.$$

This gives, within each well, eigenvalues $\lambda=0$ and $\lambda=-i3p(1+e')$ with $e'=e/3$ and eigenstates $\mathbf{v}_0,\mathbf{v}_e$. In this limit, both wells are completely separated.

(2) We now assume that the orientation rate between the wells is low; that is, $\omega_{e0}<|\omega_1-\omega_3|$ and $\omega_{e1}<|\omega_2-\omega_4|$. Then, we write for the first well the magnetic operator containing the resonance frequencies in

the basis $\mathbf{v}_0, \mathbf{v}_e$ as

$$\frac{1}{f(1+e')}\begin{bmatrix} -f(e'\omega_1+\omega_2) & (\omega_2-\omega_1)/\sqrt{2} \\ \sqrt{2}e'f^2(\omega_2-\omega_1) & -f(\omega_1+e'\omega_2) \end{bmatrix},$$

where $f=[1+(e')^2]^{-1/2}$, and identically for the second well.

It is not difficult to prove that only the $\lambda=0$ eigenvalue of $\tilde{K}$ contributes to the EPR spectrum in this limit of total average between ground and excited state, so that we select just the (1,1) element of the above matrix. Then two resonances (one for each well) will be seen, at frequencies

$$\frac{\omega_1+3\omega_2\exp(-\Delta/kT)}{1+3\exp(-\Delta/kT)} \text{ and } \frac{\omega_3+3\omega_4\exp(-\Delta/kT)}{1+3\exp(-\Delta/kT)} . \tag{3}$$

This is the result expected when the system undergoes fast transitions within states with different SH parameters: the frequency shifts from the ground state-one, ω_1, to an average of ω_1 and ω_2, the weight of each frequency being their relative population probabilities at equilibrium.[9] If, on the contrary, the transition $1\leftrightarrow 2$ were very slow both spectra would appear separately, the one corresponding to the excited state growing at the expenses of the ground-state one as temperature increases.

(3) Now we introduce, in the same basis, the reorientation matrix connecting both sites,

$$\tilde{\Gamma}=\frac{1}{f(1+e')}\begin{bmatrix} \tilde{M} & -\tilde{M} \\ -\tilde{M} & \tilde{M} \end{bmatrix},$$

where

$$\tilde{M}=i\begin{bmatrix} -f(e'\omega_{e0}+\omega_{e1}) & (\omega_{e1}-\omega_{e0})/\sqrt{2} \\ e'f^2(\omega_{e1}-\omega_{e0}) & -f(\omega_{e0}+e'\omega_{e1}) \end{bmatrix}.$$

Again, as for the magnetic part, only the (1,1) element will contribute in the average limit, with an effective frequency

$$\frac{\omega_{e0}+3\omega_{e1}\exp(-\Delta/kT)}{1+3\exp(-\Delta/kT)} .$$

This is the result for the tunnel-controlled process via an excited state.[6] We see that, through thermal excitation, the defect can reorient at a frequency much higher than the one corresponding to the ground state.

(4) If, on the contrary the reorientation process is such that $\omega_{e0}>\delta_0$ and $\omega_{e1}>\delta_e$, then the perturbative order between 2 and 3 must be altered. Omitting the details of the calculation, the result is that a thermal average is again obtained between resonance frequencies but now a single resonance is observed, at

$$\frac{\omega_{gr}+3\omega_{ex}\exp(-\Delta/kT)}{1+3\exp(-\Delta/kT)} ,$$

where

$$\omega_{gr}=(\omega_1+\omega_3)/2 ,$$
$$\omega_{ex}=(\omega_2+\omega_4)/2 .$$

We now get a thermal average of the orientational averaged signals. In first order, neither p nor ω_e contribute to the linewidth. In second order, they give a term proportional to the thermal average anisotropy and inversely proportional to the average transition probability. In intermediate cases a numerical calculation must be done.

C. Computer simulations

In order to illustrate some of the many possibilities encountered depending on the relative magnitude of the parameters involved, we have considered a defect with the interactions and parameters similar to those of H_i^0(Li). In this defect, the paramagnetic spin interacts with two nuclei: H ($I=\frac{1}{2}$) and Li ($I=\frac{3}{2}$). We only show throughout the paper the "high-field" spectrum which corresponds approximately to $m_H=-\frac{1}{2}$.

We have taken as ground-state parameters those de-

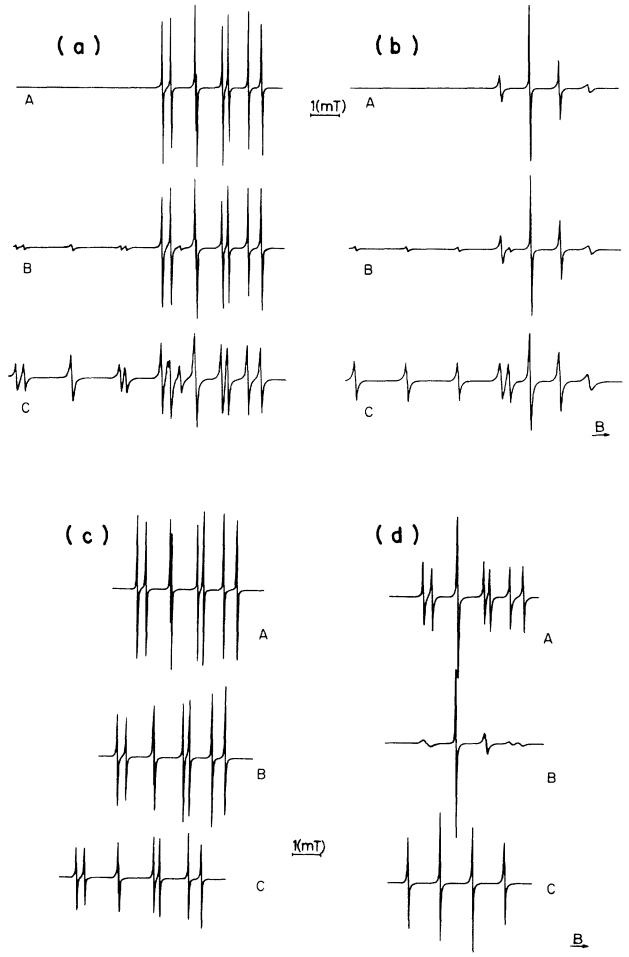

FIG. 2. Spectra calculated for cases numbered 1 to 4 in Sec. III C. The parameters are (K and ω_e's in MHz) the following. (a) Case 1: $K=1$, $\omega_{e0}=0$, $\omega_{e1}=0$. *A*: 29 K; *B*: 57 K; *C*: 115 K. (b) Case 2: $K=1$, $\omega_{e0}=10$, $\omega_{e1}=500$. *A*: 29 K; *B*: 57 K; *C*: 115 K. (c) Case 3: $K=10^4$, $\omega_{e0}=0$, $\omega_{e1}=0$. *A*: 29 K; *B*: 57 K; *C*: 115 K. (d) Case 4: $K=10^4$, $\omega_{e0}=0$, $\omega_{e1}=500$. *A*: 21.5 K; *B*: 29 K; *C*: 57 K.

rived from the static spectrum.[4] For the excited state, the isotropic hyperfine (hf) parameters are derived from the temperature evolution of the splitting observed, assuming that an expression of type (3) is valid. Since our calculations give a small dynamic contribution to the dipolar hf constant value (6%), the anisotropy of the excited state has been taken equal to that of the ground state. Equation (2) has been written in the basis $|j,\pm,m_{\mathrm{Li}},m_{\mathrm{H}}\rangle$ where $j=1,\ldots,4$ HO levels (two in each site), $\pm$ represent the magnetic sublevels with $m_s=\pm\frac{1}{2}$; $m_{\mathrm{Li}}=\pm\frac{3}{2}$, $\pm\frac{1}{2}$ are the ^{7}Li third component of nuclear spin moment, and $m_{\mathrm{H}}=\pm\frac{1}{2}$.

Four representative cases can be distinguished.

Case 1. Slow thermal excitation (K small) and reorientation rates ($\omega_{e0}\ll\delta_0$, $\omega_{e1}\ll\delta_e$) [Fig. 2(a)]. The spectrum consists of a superposition of two anisotropic sets of lines corresponding to the "static" situation of the ground and excited states. As temperature increases, the excited-state spectrum grows at the expense of the ground-state one.

Case 2. Slow thermal excitation (K small) but fast reorientation rates ($\omega_{e0}\gg\delta_0$, $\omega_{e1}\gg\delta_e$) [Fig. 2(b)]. The spectra of case 1 are now averaged. Two sets of lines corresponding to the averaged excited and ground states are now found.

Case 3. Slow reorientation but fast thermal excitation rates. K is high and $\omega_{e0}\ll\delta_0$, $\omega_{e1}\ll\delta_e$ [Fig. 2(c)]. Only one anisotropic spectrum is seen with parameters corresponding to the thermal average of the ground- and excited-state ones. As temperature increases the narrow lines shift towards the positions of the average spectrum. The average is within each potential well so the anisotropy is conserved.

Case 4. Fast thermal excitation and reorientation only through the vibrational excited states. K is high, $\omega_{e0}=0$, $\omega_{e1}\gg\delta_e$ [Fig. 2(d)]. Though the defect does not reorient at low temperatures (and thus it shows an anisotropic spectrum) it does as T increases, through the excited level, until an isotropic spectrum is seen. Moreover, the isotropic parameter of the averaged spectrum increases from the ground-state one to a mean value with a temperature-dependent weight factor. This is the case closest to our experimental situation, so that we will try to fit the spectra in these conditions. For this purpose we define an averaged excitation rate $1/\tau$ as

$$1/\tau=3[W_{12}+\exp(-\Delta/kT)W_{21}]/[1+3\exp(-\Delta/kT)]\ . \tag{4}$$

IV. APPLICATION TO H_i^0(Li) AND D_i^0(Li) IN CaO

The defect production procedure, stability, and interpretation of the low-temperature EPR spectra of H_i^0(Li) and D_i^0(Li) defects in CaO as well as the spin-Hamiltonian parameters for both defects have been previously reported in Ref. 4 and we will not produce them here. The evolution of the EPR spectra with temperature is given in Fig. 3. Since most prominent changes occur when the splittings between the hyperfine lines corresponding to different sites are larger, we will study the $\mathbf{H}\|[110]$ spectra. This orientation also has the advantage of the negligible pseudosecular contributions to the spectra as compared with the secular ones, which justifies the use of a secular approach.

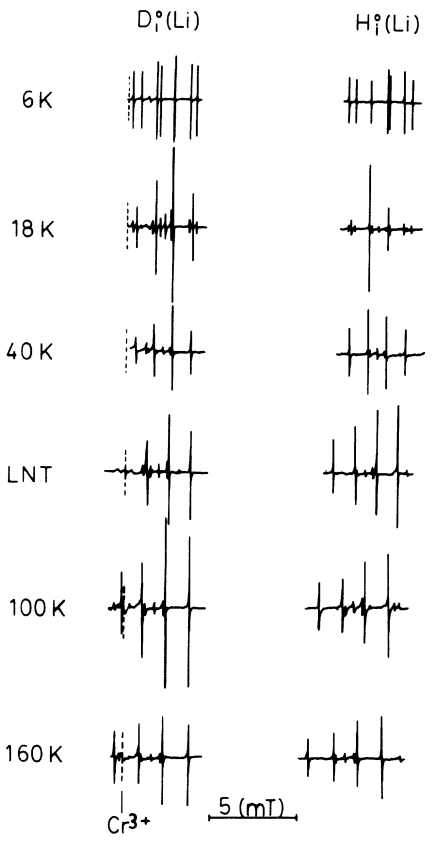

FIG. 3. Evolution of the [110] experimental spectra of D_i^0(Li) and H_i^0(Li) as a function of temperature. The vertical scale is not the same for all spectra.

We summarize briefly the remarkable experimental facts in the [110] spectrum: Two dynamic stages can be distinguished in the temperature evolution.

(1) In the first one, the anisotropy is averaged and an isotropic line appears in the middle of the anisotropic ones. The temperature of appearance is lower the smaller the anisotropy. As T increases, the central line grows at the expense of the anisotropic spectrum, which also seems to start an averaging process. However, the spectrum is lost before the averaging is completed. When comparing H_i^0(Li) and D_i^0(Li) we see that this process occurs at lower temperatures in the D_i^0(Li) case, indicating that the effective reorientation frequency is higher for this defect (inverse isotope effect). This proves that the reorientation is taking place through the excited state, which lies closer in D_i^0(Li) than in H_i^0(Li). For this effect to be observed, as discussed in Sec. III, it is required (and one would expect so) that the reorientation in the excited state be faster than in the ground state. The sudden appearance of a central line, instead of a gradual averaging of the anisotropy, is not reproduced by the simulations,

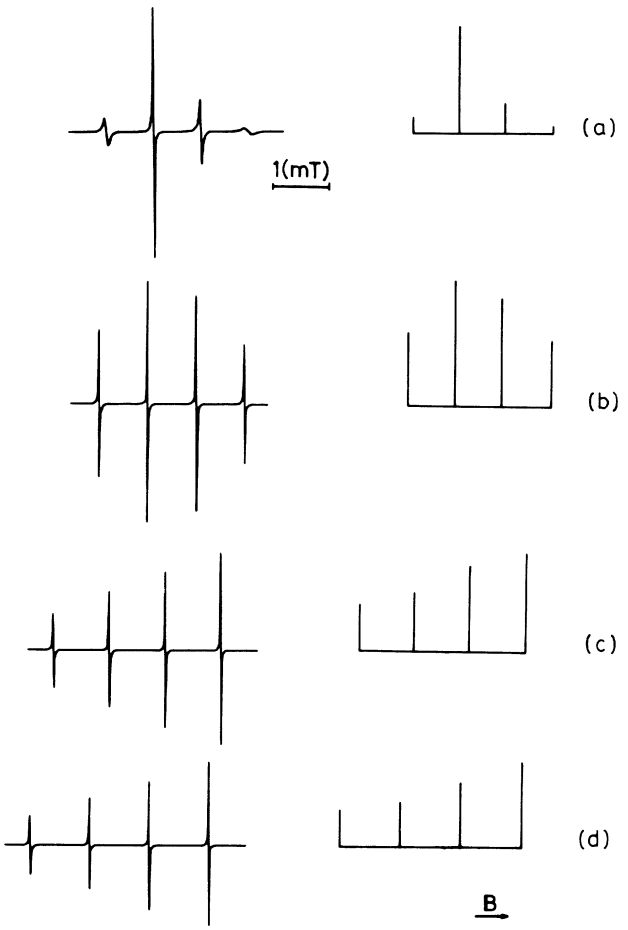

FIG. 4. Fitting of the calculated spectra (left) to the H_i^0(Li) experimental ones (right). Only the line positions and intensities are shown for the latter. Parameters are $\Delta=120$ cm^{-1}, $K=8000$ MHz. (a) 23 K, $1/T_2=0.5$ MHz. (b) 40 K, $1/T_2=0.3$ MHz. (c) 77 K, $1/T_2=0.2$ MHz. (d) 100 K, $1/T_2=0.2$ MHz.

and will be discussed later on.

(2) At temperatures of about 40 K a single hf spectrum is observed for each defect, though the intensity pattern is not completely isotropic. Above this temperature the hf parameters increase due to the thermal population of the excited state. For fast transitions between both states ($1/\tau \gg |a_1-a_2|$) an average parameter is observed at each T, but the value of this average varies with T in the form expressed in (3).

We have attempted to reproduce all these features in our calculations, taking positions and relative intensities as fitting criteria. In order to reduce the dimensions, only diagonal Hamiltonian terms have been retained. This amounts to neglecting the effect of nonsecular (nsc) and pseudosecular (psc) terms in the line shape. However, inasmuch as we limit ourselves to the [110] spectrum, in which the secular effects are strong, this will not be very important. On the contrary, psc effects are dominant in the [100] spectrum at the first stage of averaging. In both directions, psc effects disappear when the anisotropy is averaged out. nsc terms, on the other hand, are present in the isotropic part of the hf interaction and can thus have an influence even in the averaged spectra. The use of the secular approach also allows us to simulate the eight-site defect reorientation by the two-well model discussed above. This amounts, as shown in previous works, to neglecting the broadening effect of some (not all) pseudosecular terms. Since we are using a completely secular approach this problem is irrelevant. There is, however a distinction when one wants to compare the ω_e's obtained through both models: The total reorientation frequency (from one site to any other) is the same in both cases, but the particular frequency for the motion from one site to one of the others will be four times higher in the two-site model than in the eight-site one.

As an example, in Fig. 4 we show the calculated [110] spectra for H_i^0(Li) as a function of the temperature. Similar calculations are performed for D_i^0(Li). In Table I, we give the parameters resulting from the fitting and the τ's obtained from K according to the definition in (4). The values at 100 K are in good agreement with those obtained in Ref. 4 from relaxation theory. The temperature dependence of τ is fixed by the Bose factors, whereas that of the jump frequencies is, in principle, unknown. In that table we indicate in parentheses the temperatures at which it has been possible to determine the value of the corresponding parameter.

V. DISCUSSION AND CONCLUSION

We shall now discuss the sensitivity of the method in each stage to the parameters involved.

At low temperatures the most prominent effects are due to thermally activated reorientation, either in the ground state (ω_{e0}) or through the excited state (ω_{e1}). A small but nonzero reorientation must be included in the ground state in order to fit the spectra. As shown in Table I, $\omega_{e0}(D_i^0(\text{Li}))$ is smaller than $\omega_{e0}(H_i^0(\text{Li}))$ at 23 K (at higher temperatures the effect of ω_{e0} is overwhelmed by that of ω_{e1}). This is the usual isotope effect, according to which slower jump rates are expected for heavier de-

TABLE I. Parameters obtained from the fitting: K, ω_{e0}, ω_{e1}, $1/T_2$ in MHz, τ in s and Δ in cm^{-1}.

	K	τ	ω_{e0} (23 K)	ω_{e1} ($T\leq 40$ K)	$1/T_2$	Δ
H_i^0(Li)	8000±2000	3.8×10^{-8} (23 K) 1.5×10^{-10} (100 K)	4	8000	0.5 (23 K) 0.2 (100 K)	120±10
D_i^0(Li)	2700±700	3.2×10^{-8} (23 K) 3.4×10^{-10} (100 K)	2	6000	0.7 (23 K) 0.2 (100 K)	100±10

fects. Nevertheless, D_i^0(Li) is at a higher stage of averaging than H_i^0(Li), as a consequence of the earlier population of the excited state, where the reorientation is much faster than in the ground state. This is known as inverse isotope effect.

At temperatures above 50 or 60 K the spectra are no longer sensitive to the ω_e's and the intensity pattern is entirely due to thermal excitation (K) and intrinsic relaxation ($1/T_2$).

From the intensity at high temperatures, an interval can be fixed for K (or, equivalently, for $1/\tau$), once the intrinsic linewidth parameter $1/T_2$ has been determined, for instance, from the completely averaged spectrum. At the same stage of averaging, lower probabilities are needed for D_i^0(Li), except at very low temperatures. That is, τ will be longer. In fact, a factor of 3 is found between $K(H_i^0(\text{Li}))$ and $K(D_i^0(\text{Li}))$. This value fulfills the $M^{-3/2}$ law given by the phonon density of states and transition probabilities for a HO-type dependence for Δ, which is, within error, the experimental result. At very low temperatures, however, the effect of a higher K, which favors excitation, is compensated by the small phonon occupancy number due to the greater gap, so that longer τ are obtained for H_i^0(Li) than for D_i^0(Li), as shown in Table I.

The values given in Table I have large errors, for the experimental intensities (or linewidths) are very sensitive to factors such as overmodulation, saturation, etc. This can be the reason why higher $1/T_2$ are needed at low temperatures. Since at very high temperatures the linewidth is dominated by intrinsic processes, small changes in $1/T_2$ can also affect the value of τ in almost an order of magnitude.

As a conclusion, we can say that our work confirms the model of the H_i^0(Li) and D_i^0(Li) dynamics, whose most striking aspect is the inverse isotope effect, a consequence of the reorientation via an excited state.

Finally, some words must be said about the sudden appearance of a peak in the averaged positions, instead of the gradual coalescence usually observed. In fact, this feature is not reproduced within our model and we must assume an extra hypothesis, such as sample inhomogeneity resulting in a distribution of sites, which would imply a distribution of Δ or, equivalently, of jump frequencies ω_e's for the same temperature.

With respect to the applicability of this method to other cases, we can affirm that line-shape simulation is best if one wants to reproduce all the details of the experimental spectra. Within our formalism, factors such as the anisotropy contribution to the line shape at intermediate temperatures are much easily handled than, for instance, in relaxation matrix theories. If the Hamiltonian is appropriately chosen it can also account for pseudosecular and nonsecular broadening. It is easy to see that in the limit of fast reorientation and neglecting anisotropy, relaxation theory is equivalent to developing the Liouville operator of our formalism up to second order.

ACKNOWLEDGMENTS

This work was done with financial support from the Dirección General de Investigación Científica y Técnica under Contract No. PB 0361 with the Consejo Superior de Investigaciones Científicas.

[1]M. L. Sanjuán and V. M. Orera, J. Phys. C **19**, 67 (1986).
[2]V. M. Orera and M. L. Sanjuán, Phys. Rev. B **33**, 3058 (1986).
[3]V. M. Orera, M. L. Sanjuán, and M. M. Abraham, J. Chem. Phys. **88**, 2976 (1988).
[4]V. M. Orera, P. J. Alonso, M. L. Sanjuán, and R. Alcalá, Phys. Rev. B **39**, 7928 (1989).
[5]J. A. Sussman, J. Phys. Chem. Solids **28**, 1643 (1967).
[6]V. S. Vikhnin, Fiz. Tverd. (Leningrad) **20**, 1340 (1978) [Sov. Phys. Solid State **20**, 771 (1978)].
[7]K. Murakami, H. Kuribayashi, and K. Masuda, Phys. Rev. B **38**, 158 (1988).
[8]J. Haupt, Z. Naturtorsch. Teil A **26**, 1575 (1971).
[9]J. H. Freed and G. K. Fraenkel, J. Chem. Phys. **39**, 326 (1963); G. K. Fraenkel, *ibid.* **42**, 4275 (1965).